Molecular Crystals and Liquid Crystals
Publication details, including instructions for authors and subscription information:
http://www.tandfonline.com/loi/gmcl18

Study of Tails in Smectic Liquid Crystals. I. The Effect of Fluorocarbon/Hydrocarbon Ether Tails on Phenyl Ester Biphenyl Cores

Y. H. Chiang [a], A. E. Ames [a], R. A. Gaudiana [a] & T. G. Adams [a]
[a] Polaroid Corporation, Cambridge, MA, 02139
Version of record first published: 24 Sep 2006.

To cite this article: Y. H. Chiang , A. E. Ames , R. A. Gaudiana & T. G. Adams (1991): Study of Tails in Smectic Liquid Crystals. I. The Effect of Fluorocarbon/Hydrocarbon Ether Tails on Phenyl Ester Biphenyl Cores, Molecular Crystals and Liquid Crystals, 208:1, 85-98

To link to this article: http://dx.doi.org/10.1080/00268949108233946

Mol. Cryst. Liq. Cryst., 1991, Vol. 208, pp. 85–98
Reprints available directly from the publisher
Photocopying permitted by license only

Printed in the United States of America

Study of Tails in Smectic Liquid Crystals. I. The Effect of Fluorocarbon/Hydrocarbon Ether Tails on Phenyl Ester Biphenyl Cores

Y. H. CHIANG, A. E. AMES, R. A. GAUDIANA and T. G. ADAMS
Polaroid Corporation, Cambridge, MA 02139

(Received June 19, 1991)

The use of the mixed fluorocarbon/hydrocarbon ether sequence [1H,1H,5H-octafluoro-1-pentoxy-]ethoxy in place of aliphatic or aliphatic ether sequences significantly enhances the temperature range of the chiral smectic C (Sc*) liquid crystalline phase. Considerations derived from the literature, supported by computer modeling, suggested that stabilization of the Sc* phase results from enhancement of the population of gauche conformers. These considerations have led to liquid crystal molecules with the widest range of Sc* phase thus far reported.

INTRODUCTION

The work described here was initiated to find ferroelectric liquid crystal molecules for use in advanced electro-optical devices. In this paper we adopt the model that liquid crystal molecules have three segments, the "tail," the "core," and the "head," as shown in Figure 1.

Many characteristics of molecules have been considered to cause or enhance the Sc* phase. These include molecular dipoles and polarizabilities[1] arising predominantly from the core segment, configurational states[2] arising predominantly from the tail and/or head segments, and the overall packing characteristics of the molecules. The design of core and chiral head moieties have been extensively investigated.[3–8] Polyether tails with 2 or 3 oxygen atoms have been investigated[9,10,41] and found to enhance smectic phase formation over all hydrocarbon tails.

It is frequently assumed that the Sc* phase arises from intermolecular electrostatic interactions. For example, Macmillan's prediction[1] of the ferroelectric Sc* phase was based on analysis of dipolar interactions, and this model was cited by Meyer

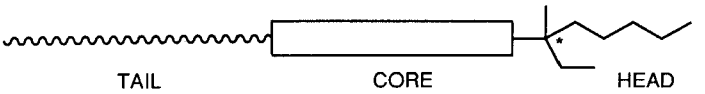

FIGURE 1 The rigid center is designated as core, the branched chiral aliphatic chain as head, and the straight long chain as tail.

et al.[11] Various anisotropies have been considered,[12-13] some of which were reviewed by Cotter.[14] Alkoxy benzoic acids have been shown by Demus, et al.[15] to have Sc behaviour, as further elaborated by Cser.[16] These compounds have been shown by Bryan, et al.[17] to be symmetrical hydrogen bonded dimers, which therefore have no net dipole.

Using monte-carlo models Frenkel[18] has shown that excluded volume factors alone can lead to a smectic A state, and Dowell's modeling[2] has indicated that conformational and steric considerations may be sufficient to explain smectic states in general. Assuming that steric factors stabilize smectic states, the particular molecular features which enhance the Sc* must still be selected and optimized.

Considering particularly the significance of tail segments on the Sc* phase, there are numerous examples where increasing aliphatic tail length to more than 5 carbon atoms induces either Sc or Sc* phases.[10,11,19,20,21] Such lengths are well beyond those where additional carbon atoms would be expected to affect the core segment. Correlations between the Sc* transition temperatures and the number of carbon atoms for simple n-alkoxy tail[19,22,23] as well as a branched alkoxy tail[24] have been established. Goodby, et al.[25] has shown several examples where mixtures of compounds differing only in aliphatic tail length exhibit Sc behavior which is absent in the pure compounds.

There is experimental evidence that the Sc* state is associated with a large population of gauche isomers[26] in the aliphatic segments. Galbiati and Zerbi,[27] Fanelli, et al.,[28] Zabon et al.,[29] Bos et al.,[30] and Bryan et al.,[31] have all found evidence for a significant level of gauche isomers in the smectic C phase. Watanabe and Kriegbaum[32] established that destabilizing the crystalline phase stabilizes the smectic state, which argument is consistent with the need for gauche isomers. NMR investigations[17,27,29] show that hydrocarbon tails in the smectic phases are conformationally disordered but on the NMR time scale are rapidly interconverted. We take the above arguments to indicate that the tendency of the tails to support gauche conformers plays a significant role in maintaining the stability of the Sc* phase relative to other phases.

RESULTS

This investigation was carried out along two lines. The first is synthesis and examination of compounds with tails chosen to have a high population of gauche isomers. We report here the effect of a fluorocarbon/hydrocarbon hybrid tail, i.e. [1H,1H,5H-octafluoro-1-pentoxy-]ethoxy. The Sc* phase range of this tail has been investigated with several heads attached by an ester group to three different three-ring cores, all of which have phenyl and biphenyl rings linked to each other by an ester group.

The second line of investigation was a modeling exercise to confirm that the observed differences arise from variations in conformational states, and to better picture what particular conformational states may ultimately be of greatest value in promoting the Sc* phase.

For comparison with the hybrid tail, we have selected aliphatic hydrocarbon and

polyether tails. In all of the compounds reported the backbone of the tail has nine atoms including an oxygen atom linking the tail to the core. The structures of the compounds are given in Table I, and the synthesis of representative compounds are shown in Scheme I and described in greater detail in the experimental section.

Data on the phase transition temperatures for compounds separately containing all three tails is presented in Table II and Table III, and in Figure 4 and Figure 5 graphically.

Concurrent with, and as a guide to, synthesis, modeling of candidate tails was initiated to estimate the relative tendency of each type of tail to occupy gauche states. We calculated the minimum energy geometry and enthalpy of the $243 = 3^5$ conformers of each of three model tails using MNDO. MNDO[33,34] was chosen

TABLE I

Notations for chemical structures

STRUCTURE	TYPE	NOTATION
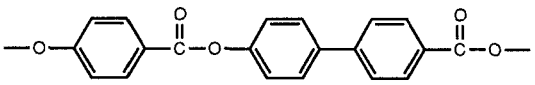	CORE	**PEPP**
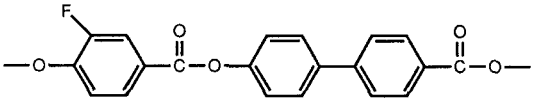	CORE	**PFEPP**
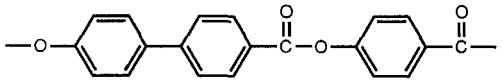	CORE	**PPEP**
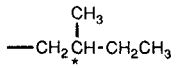	HEAD	**C4***
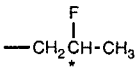	HEAD	**C3F***
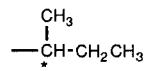	HEAD	**C3***
$-CH_2CH_2CH_2CH_2CH_2CH_2CH_2CH_2CH_3$	TAIL	**C8**
$-CH_2CH_2OCH_2CH_2OCH_2CH_3$	TAIL	**EO**
$-CH_2CH_2OCH_2(CF_2)_4H$	TAIL	**HY**

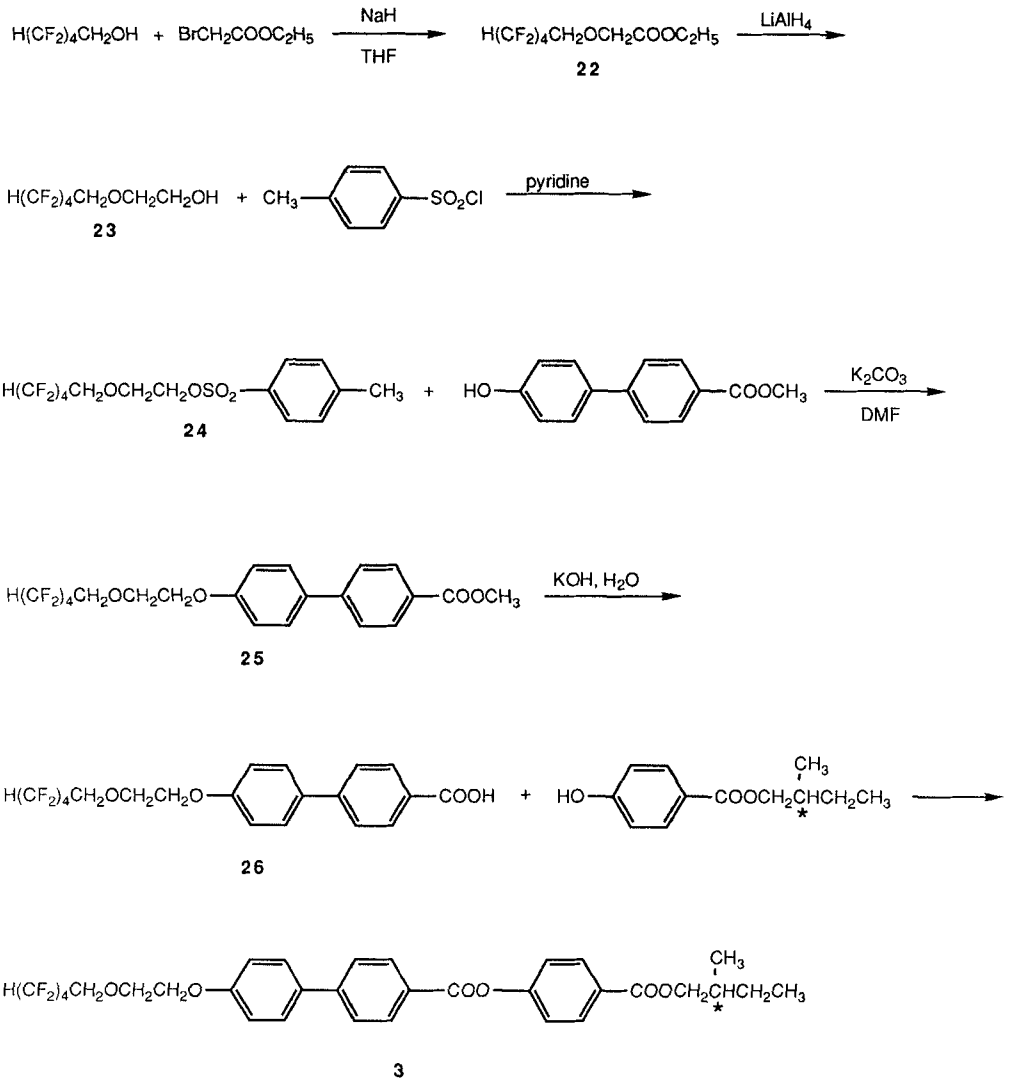

SCHEME I Synthetic route for **3**

as the computational method to avoid any bias, i.e., toward crystal formation, that might be inherent in molecular mechanics parameterization. To satisfy computational constraints, the judgement was made that a 5 atom chain would indicate at least qualitatively the phenomena to be expected from the longer chains.

DISCUSSION, EXPERIMENTAL

The dramatic increase in Sc* temperature range arising from the hybrid tail, as compared to the aliphatic, or aliphatic ether tail, can be seen in Table III. The

TABLE II

Phase transition temperatures

	Head	Core	Tail	COOLING, °C: I→S_A	I→Ch	Ch→S_A	S_A→S_C*		S_C*→K	HEATING, °C: K →S_C*	S_C* →S_A
1	C4*	PPEP	C8	187	-	-	141	-	63	70	142
2			EO	140	-	-	85	-	29	32	86
3			HY	165	-	-	141	-	22	64	142
4	C3F*		C8	210	-	-	90	-	68	83	92
5			EO	176	-	-	64	(# 1)	42	60	66
6			HY	213	-	-	119	-	61	87	118
7	C3*		C8	179	-	-	132	-	45	83	133
8			EO	129	-	-	69	-	39	43	69
9			HY	159	-	-	140	-	24	81	141
10	C4*	PFEPP	C8	-	156	150	119	-	73	101	119
11			EO	-	94	86	72	-	24	- (# 2)	-
12			HY	141	-	-	109	-	15	75	110
13	C3F*		C8	184	-	-	-	-	68	- (# 3)	-
14			EO	-	139	134	82	-	35	64	82
15			HY	197	-	-	93	-	30	69	94
16	C3*		C8	140	-	-	-	-	92	- (# 4)	-
17			EO	71	-	-	65	-	62	- (# 5)	-
18			HY	136	-	-	113	-	11	72	114
19	C4*	PEPP	C8	-	171	164	117	-	50	86	117
20			EO	-	112	92	77	-	43	- (# 6)	-
21			HY	156	-	-	135	-	0	76	136

(# 1) Other smectic states observed at 42° and 32°, with smectic →K @ 12°.
(# 2) K→S_A @ 75°, S_A→Ch @ 87°
(# 3) K→S_A @ 107°
(# 4) K→S_A @ 114°
(# 5) K→I @ 83°
(# 6) K→S_A @ 84°; S_A→Ch @ 93°

TABLE III

Sc* phase temperature ranges

	Head	Core	COOLING, °C: Tail C8	EO	HY	HEATING, °C: Tail C8	EO	HY	SUPER COOLING, °C: Tail C8	EO	HY
1,2,3	C4*	PPEP	78	56	119	72	54	78	7	3	42
4,5,6	C3F*		22	22	58	9	6	31	15	18	26
7,8,9	C3*		87	30	116	50	56	60	38	4	57
10,11,12	C4*	PFEPP	46	48	94	18	-	35	28	-	60
13,14,15	C3F*		-	47	63	-	18	25	-	29	3
16,17,18	C3*		-	3	102	-	-	42	-	-	61
19,20,21	C4*	PEPP	67	34	135	31	-	60	36	-	76

FIGURE 2A Stereo pairs showing the location of the end carbons for the 231 conformers of model tail T1, the chain containing ethers and flourine substituents. Taking the Z axis along the HO bond, the location of the terminal carbon is plotted with X and Y in plane, and Z out of the plane. The origin of the X-Y plane is located by a "+." The cross, "×," locates the terminal carbon of the all trans, all carbon chain, T3. The area of the dots plotted at each location is weighted roughly as a Boltzman distribution at 25°C. The total number of pixels plotted in these figures is approximately the same, although the graphic accuracy of the plots is low. The degree of left-right symmetry is an indication of the reliability of the calculation since all conformers were calculated without regard to symmetry. In a real molecule the attachment of the chain to the core (with a core atom replacing the terminal hydroxyl hydrogen) would be subject to rotation, for these figures in the plane of the paper.

FIGURE 2B As in Figure 2A for the 240 conformers of chain T2, the ether containing chain. The highly twisted but stable conformers which place the terminal carbon close to the HO could not exist in longer chains.

FIGURE 2C As in Figure 2A for the 240 conformers of chain T3, the all CH2 chain. Comparing with Figure 2A, the all CH2 chain is much more likely to be in a "straight," or all trans configuration than the chains with ether.

range of Sc* is enhanced both in heating and cooling cycles. For every example listed, the Sc* range of the compound containing the hybrid tail is larger than either of its homologs with the other tails.

As expected, the magnitude of the stabilization of the Sc* range also depends on the structure of the core and to a lesser extent on the chiral head. For example, in the biphenyl-phenyl core, the hydrocarbon tails are more effective in stabilizing the Sc* phase than the hydrocarbon ethers, but in the phenyl-biphenyl core the latter are generally more effective.

A comparison of **1, 2** and **3** with **19, 20**, and **21** shows that any of the tails directly attached to the biphenyl ring exhibit a larger Sc* phase.

It should be noted that the hybrid tail is less sensitive to changes in the core or the chiral head. For example, the placement of a fluorine atom on the chiral carbon in the head group, e.g., **4–6** and **13–15**, significantly decreases the Sc* range of **4**

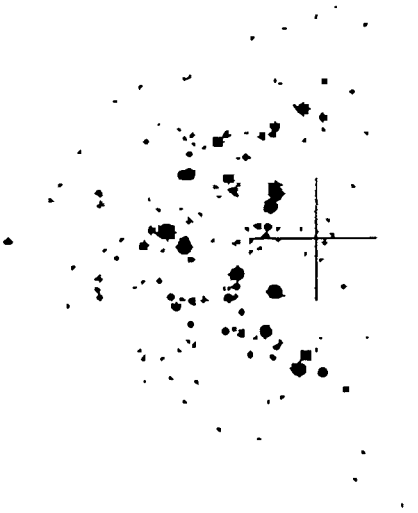

FIGURE 3A A two dimensional diagram indicating the distribution of dihedral angles found in the calculation for tail T1. Plotted are the same weighted dots as in Figure 2, but with the X value as the sum of the cosines of the 5 dihedral angles, Q_i, and Y as the sum of the sines: $X = \Sigma \cos(Q_i)$, and $Y = \Sigma \sin(Q_i)$.

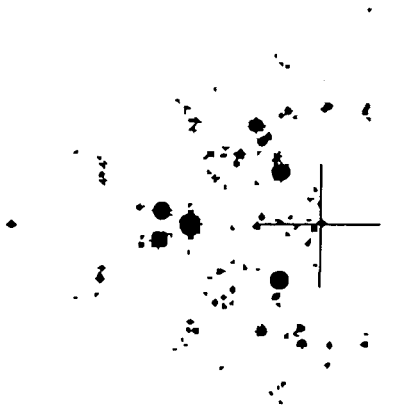

FIGURE 3B As in 2A for tail T2.

and **5**, and **13** does not exhibit any tilted phases but **6** and **15** are relatively unaffected. In addition, compounds **10–18** contain a fluorinated core, which should significantly alter the resultant dipole, but the hybrid tailed compounds still exhibit a minimum Sc* range of 20°C while its homologs exhibit little or no Sc* phase. In **17** liquid crystallinity is completely absent.

An outcome of this work that was anticipated as to kind, but not to extent, was the large supercooling demonstrated by the hybrid tails. We rationalize this result as follows.

Since the rotational barrier of an —O—CH_2— bond is approximately 1.5 kcal/

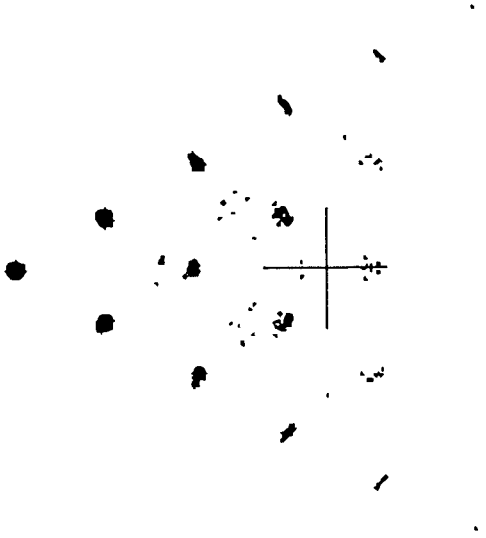

FIGURE 3C As in 2A for tail T3.

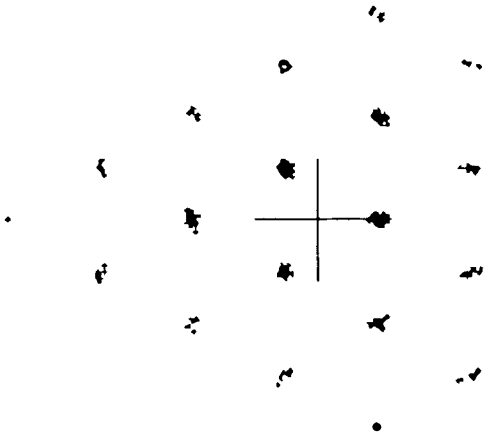

FIGURE 3D The same mathematical basis as the diagrams in 3A–C, but with equal probability of dihedrals from the set −60, +60, 180, individually subject to a random perturbation up to +/− 4 degrees to effect separation of the plotted circles.

mol[26,35,36] compared to 3.5 kcal for —CH_2—CH_2—, hydrocarbon ethers interconvert more rapidly than the hydrocarbons. Steric considerations indicate that the introduction of fluoromethylene sequences should give higher rotational barriers than the hydrocarbon tails. Assuming that the rotational barriers dictate the rate at which one phase can interconvert to another, the ordering of supercooling should then be hybrid > hydrocarbon > ether. This trend is supported by the results shown in Table III.

Observations incidental to those reported here indicate that the conformation of tail moieties in smectic compounds also affects their propensity to align on oriented surfaces. It has been generally observed that liquid crystalline compounds

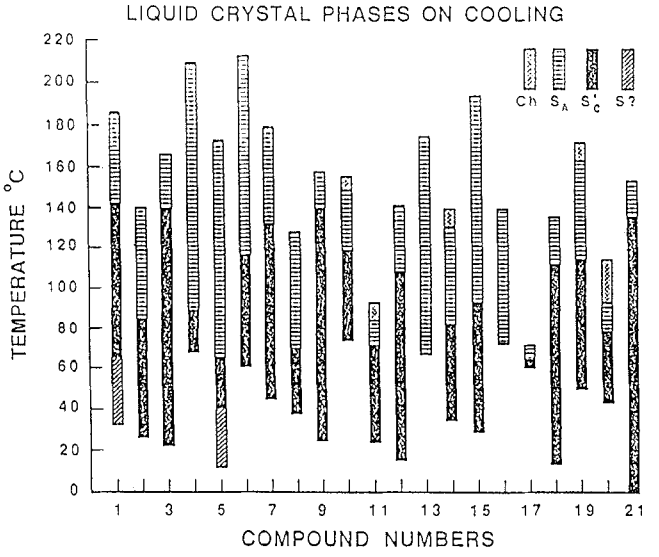

FIGURE 4 Phase transition temperatures for compound 1 thru 21 at cooling rates at 10°C/min. S? designates smectic phases higher ordered than Sc* and Ch designates the cholesteric phase.

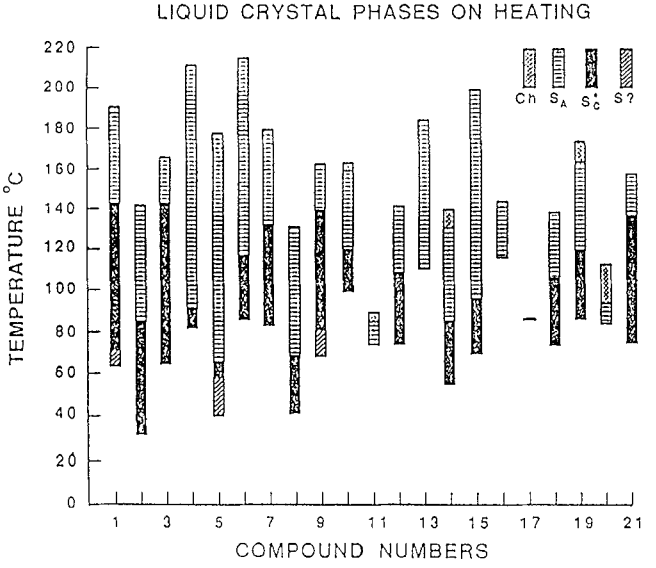

FIGURE 5 Phase transition temperatures for compound 1 thru 21 at heating rates at 10°C/min. S? designates smectic phases higher ordered than Sc* and Ch designates the cholesteric phase.

containing a hydrocarbon tail exhibit homogeneous alignment on buffered polymer surfaces. Homogeneous alignment of the hybrid-tailed liquid crystals can be readily achieved on buffed polymer surfaces. On the other hand, many of the polyether-tailed compounds prefer homeotropic alignment, and as a result have limited utility

in device applications where high order parameters are required. Polyether-tailed compounds can, however, be used in multicomponent mixtures.[37,38]

DISCUSSION, CALCULATION

The results of the calculations are shown in Table IV, which lists the thermally weighted average number of non-trans bonds found for each type of tail. For isoenergetic gauche and trans conformers, neglecting self-intersections, the average number of non-trans bonds would be 3⅓.

For the model tails in Table IV, the ordering of the population of gauche states per chain is T1 > T2 > T3. These tails are analogs of the HY, EO, and C8 tails in Table I. From Table III, the domain of Sc* is greater for the tail HY than for either EO or C8 in all cases. While the fraction of gauche states calculated for the model chains parallels the observed Sc* behaviour, additional factors must be found before complete ordering and quantitative prediction can be achieved.

The additional factors promoting the Sc state may have to do with the type of organization permitted by the tail conformational sequences. Some indication of what these sequences are can be seen in Figures 2A–3D. Stereo pairs showing the location of the terminal carbon for the various conformers are shown in Figures 2A–2C. Although the entropy of the hydrocarbon chain (T3) and the hybrid chain (T1) are within 0.1 R of each other, comparing Figures 2A and 2B it can be seen that the geometry of populated states is quite different between the two chains, as well as from T2. An alternative representation of the tail geometries is shown in Figures 3A–3C.

Shown also in Table IV are the entropy contributions from conformational states calculated for the three chains. For isoenergetic gauche and trans conformers, neglecting self-intersections, the entropy would be 5Rln3. The entropy found for the hydrocarbon chain is 5Rln2.41. How do we resolve the apparent disparity where the chain with highest entropy, T3 in Table IV, is not associated with the largest fraction of gauche isomers? The all carbon chain has as its lowest enthalpy and

TABLE IV

Results of MNDO calculations of model tails

TAIL SEQUENCE	Average Gauche Bonds per Tail	Entropy* S/R (25°C)
T1) $HO-CH_2-CH_2-O-CH_2-CF_2-CF_3$	3.15	4.34
T2) $HO-CH_2-CH_2-O-CH_2-CH_2-CH_3$	3.05	4.01
T3) $HO-CH_2-CH_2-CH_2-CH_2-CH_2-CH_3$	2.00	4.41

* The actual number of conformers used was 231 for T1, and 240 for T2 and T3.

most likely single conformer the all trans state. Replacing a CH_2 with an ether forces the lowest energy conformer to include gauche bonds. If the gauche bonds induced by the ether have much lower energy than do the gauche bonds in the all carbon chain, the number of gauche bonds per chain increases at the same time that the dispersity of state populations—and therefore the entropy—decreases.[21] The hybrid tail also includes gauche states in its low energy conformers, but the fluorine substituents have raised the enthalpy of the gauche states by steric hindrance to rotation about the CF_2-CF_2 sequence. In brief, the ether substituents enable gauche conformers, and the fluorine substituents prevent the gauche conformers from overwhelming the distribution of conformers. But the main point is to call attention to the distinction between entropy and conformation.

CONCLUSION

The hybrid tail introduces two significant effects into molecules which exhibit smectic liquid crystalline phases. Independent of the nature of the core and the chiral head, compounds containing the hybrid tail exhibit the broadest Sc* phase temperature range reported to date in both cooling and heating cycles. Secondly, compounds containing a hybrid tail exhibit unusually large supercooling of the Sc* phase.[39]

The effectiveness of the hybrid tail in inducing or extending Sc* phases is attributed to the tendency of the hybrid tail to favor gauche isomers with a high barrier to interconversion. While a large population of gauche conformers is necessarily associated with increasing entropy, entropy is not the only factor inducing and/or stabilizing the Sc phase.

EXPERIMENTAL

Phase transition data was obtained with a Perkin-Elmer DSC-7 differential scanning calorimeter at heating and cooling rates of 10° per minute. Phase texture observations were made with a Zeiss 9902 Pol microscope equipped with a Leitz hot stage.

Applicable to all of the syntheses discussed is the following apparatus. IR spectra were determined with a Nicolet 20DXC FT-IR spectrometer. ^{1}H-NMR were determined on the Varian EM-390 or Varian XL 300 spectrometers. Mass spectra were recorded on a VG 7070 double focusing mass spectrometer with EI technique. Column chromatographic separations were performed with silica gel, Baker Analyzed, 60-200 mesh, suitable for column chromatography.

Ethyl 1H,1H,5H-Octafluoro-1-pentoxy acetate (**22**). To a 100 ml THF solution of 1H,1H,5H-octafluoro-1-pentanol,[40] (28.0 g, 0.12 moles), was added 5.2 g of sodium hydride (57% mineral oil suspension) in an ice-water bath to keep the temperature below 10°C. The resulting mixture was allowed to stir for 30 min before it was added to a THF solution of ethyl bromoacetate (20.2 g, 0.12 moles). The addition

was continued at such a rate that the temperature was kept below 5°C with an ice-water salt bath. After stirring at 5°C or below for 1 hr, the mixture was left at room temperature overnight. The precipitate was removed by filtration with the aid of celite and the solvent was removed by vacuum rotary evaporation. The residue was vacuum distilled and the fraction boiling between 82–86°C at 3 mm was collected. The colorless liquid weighed 25.7 g (71%). ^{1}H-NMR ($CDCl_3$, 90 MHz): δ 1.27 (t, 3H, CH_2CH_3), δ 4.20 (m, 6H, CH_2O CH_2COOCH_2), δ 5.40, 5.92, 6.57 (t, 1H, HCF_2).

1H,1H,5H-Octafluoro-1-pentoxyethanol (**23**). To a suspension of lithium aluminum hydride (7.5 g, 0.2 moles) in 100 ml of anhydrous ether, was added **22** (23.75 g, 0.0786 moles) in 75 ml of ether at such a rate as to maintain reflux. The resulting suspension was stirred at room temperature for 3 hr and 18 ml of water was added to the reaction mixture with extreme caution. The resulting mixture was filtered and the precipitate was twice triturated with 50 ml of ether. The combined ether solution was dried over anhydrous sodium sulfate, evaporated to remove solvent and the residue vacuum distilled. The yield of pure, colorless **23** was 16.7 g (77%), b. p. 69–71°/0.2 mm ^{1}H-NMR $CDCl_3$, 90 MHz): δ 3.90 (m, 6H, $CH_2CH_2OCH_2$), δ 5.40, 5.92, 6.57 (t, 1H, HCF_2); mass spectrum, m/e 276.

1H,1H,5H-Octafluoro-1-pentoxethyl-p-toluene sulfonate (**24**). To a solution of **23** (6.5 g, 0.02355 moles) in 35 ml of pyridine was added 8.73 g (0.0457 moles) of p-toluene sulfonyl chloride slowly in order to keep the temperature below 5°C with an ice-water bath. The mixture was stirred for 1 hr then left in a refrigerator overnight. The reaction mixture was poured into 300 ml of ice water and the aqueous solution extracted with two portions each of 125 ml methylene chloride. The methylene chloride solution was washed with diluted hydrochloric acid and water. After being dried over anhydrous magnesium sulfate, the solvent was removed at a reduced pressure to give an orange residue (9.5 g). This residue was chromatographed through 50 g of silica gel using hexane/methylene (1:1) as eluent. A total of 8.7 g (86%) of the p-toluene sulfonate derivative was collected as a colorless viscous liquid. ^{1}H-NMR (CDC1, 90 MHz): δ 2.45 (s, 3H, $ArCH_3$), δ 3.84 (m, 4H, $CF_2CH_2OCH_2$), δ 4.20 (m, 2H, CH_2OSO_2), δ 5.42, 6.02, 6.60 (t, 1H, HCF_2), δ 7.32 (d, 2H, ArH), δ 7.80 (d, 2H, ArH).

Methyl 4'-[1H,1H,5H-Octafluoro-1-pentoxyethoxyl-4-biphenyl carboxylate (**25**). A mixture of **24** (4.30 g, 0.01 mole), methyl 4'-hydroxy-4-biphenyl carboxylate (2.30 g, 0.01 mole), powdered anhydrous potassium carbonate (2.80 g), and potassium iodide (300 mg) in 40 ml of DMF was heated at 125–130°C for 4 hr. The reaction mixture was poured slowly into 400 ml of ice water and stirred for 30 min. The precipitate was collected, filtered, and washed with water thoroughly. The precipitate was dissolved into 150 ml of ether and the ether solution was washed with water, dried over anhydrous magnesium sulfate, and evaporated to dryness under reduced pressure. The resulting yellow residue was triturated with 50 ml of hexane to give 3.60 g (74%), m.p. 120–123°C, of a colorless solid. ^{1}H-NMR ($CDCl_3$, 90

MHz): δ 3.48 (s, 3H, OCH3), δ 4.20 (m, 6H, $CH_2OCH_2CH_2$), δ 5.45, 6.17, 6.62 δ (t, 1H, HCF_2), δ 6.98 (d, 2H ArH), δ 7.57 (m, 4H, ArH), δ 8.08 (d, 2H, ArH).

4'-[1H,1H,5H-Octafluoro-1-pentoxyethoxy]-4-biphenyl carboxylic acid (**26**). Three grams (0.00617 moles) of **25** was dissolved into a boiling mixture of 100 ml of methanol, 5 ml of 45% aq. potassium hydroxide, and 100 ml of water. All methanol was evaporated off on a steam bath. The aqueous solution was acidified with conc. hydrochloric acid, cooled in an ice bath, and filtered to give 2.82 g (97%) of a colorless solid, m.p. 149–152°C. ^{1}H-NMR (DMSO, 90 MHz): δ 4.10 (m, 6H, $CH_2OCH_2CH_2$), δ 5.83, 6.40 (t, 1H, HCF_2), δ 6.95 (d, 2H, ArH), δ 7.52 (d, 2H, ArH), δ 7.62 (d, 2H, ArH), δ 8.00 (d, 2H, ArH).

4'-[1H,1H,5H-Octafluoro-1-pentoxyethoxy]-4'-biphenyl 4-[(S)-2-methyl-1-butyl]-benzoate (**3**). A mixture of **26** (472 mg, 1.0 mM), [(S)-2-methyl-1-butyl p-hydroxybenzoate (210 mg, 1.0 mM), 1-(3-dimethylaminopropyl)-3-ethylcarbodiimide (300 mg), and 4-N,N-dimethylaminopyridine (120 mg) in 150 ml of methylene chloride was stirred at room temperature overnight. The solvent was removed under reduced pressure and the residue was chromatographed through 40 g of silica gel using 1% methanol in hexane/methylene chloride (1:1) as eluent. The high R_F fractions were collected and recrystallized from 35 ml of hexane yielding 270 mg (41%) of a colorless solid. IR: KBr 1722, 1278 cm^{-1}. ^{1}H-NMR ($CHCl_3$, 300 MHz): δ 0.971 (t, J = 2.5 Hz, 3H), δ 1.029 (d, J = 2.2 Hz, 3H), δ 1.297 (m, 1H), δ 1.548 (m, 1H), δ 1.867 (m, 1H), δ 4.171 (m, 8H), δ 5.916, 6.090, 6.263 (t, J = 2.0 Hz, 17.3 Hz, 1H), δ 7.027 (m, 2H), δ 7.309 (m, 2H), δ 7.615 (m, 2H), δ 7.710 (m, 2H), δ 8.138 (m, 2H), δ 8.245 (d, J = 2.8 Hz, 2H); mass spectrum m/e 662.

Acknowledgments

The authors acknowledge the numerous helpful discussions with their colleagues, especially Drs. A. Naiman, H. Razavi, and R. Sinta, and the suggestions of the reviewers, and thank Polaroid Corporation for permission to publish this work.

References

1. W. L. MacMillan, *Phys. Rev. A*, **8**, 1921–1929 (1973).
2. F. Dowell, *Phys. Rev. A*, **31**, 2464–2471 (1984).
3. D. M. Walba, S. C. Slater, W. N. Thurmes, N. A. Clark, M. A. Handschy and F. Supon, *J. Am. Chem. Soc.*, **108**, 5210–5221 (1986).
4. M. F. Bone, E. Coates, G. W. Gray, D. Lacey, K. J. Toyne and D. J. Young, *Mol. Cryst. Liq. Cryst. Lett.*, **3**, 189–192 (1986).
5. J. W. Goodby and T. M. Leslie, *Mol. Cryst. Liq. Cryst.*, **110**, 175–203 (1984).
6. J. W. Goodby, J. S. Patel and E. Chin, *J. Phys. Chem.*, **91**, 5151–5152 (1987).
7. K. Terashima, M. Ichibashi, M. Kikuchi, F. Furukawa and T. Inukai, *Mol. Cryst. Liq. Cryst.*, **141**, 237–249 (1986).
8. T. Sakurai, M. Mikami, R. Higuchi, M. Honma, M. Osaki and K. Yoshino, *J. Chem. Soc., Chem. Commun.*, 978–979 (1986).
9. R. Higuchi, T. Sakurai, N. Mikamu, E. Yamamoto and K. Takeuchi, K. Jpn. Kokai Tokkyo Koho Jap. Patent 63-33, 349 (1986).

10. A. C. Griffin and J. E. Johnson, Eds., "Liquid Crystals and Ordered Fluids," **4**, pp. 6, (Plenum Press, New York, 1982).
11. R. B. Meyer, L. Lieberg, L. Strzelecki and P. Keller, *J. Physique. Lett.*, **36**, 69–71 (1974).
12. W. J. A. Goossens, *Mol. Cryst. Liq. Cryst.*, **150b**, 419–445 (1987).
13. N. K. Sanyal, S. N. Tiwari and M. Roychoudhry, *Mol. Cryst. Liq. Cryst.*, **140**, 179–193 (1986).
14. M. A. Cotter, *Mol. Cryst. Liq. Cryst.*, **97**, 29–47 (1983).
15. D. Demus, H. Demus and H. Zaschke. Flussige Kristallen in Tabellen. Deutsch Vrlg. Grundstoffindustrie, Liepzig (1974).
16. A. C. Griffin and J. E. Johnson, Eds., "Liquid Crystals and Ordered Fluids," **4**, pp. 945, (Plenum Press, New York, 1982).
17. R. F. Bryan, P. Hartley, R. W. Miller and M. Shen, *Mol. Cryst. Liq. Cryst.*, **62**, 281–310 (1980).
18. D. J. Frenkel, *J. Phys. Chem.*, **91**, 4912–4916 (1987); D. J. Frenkel, **92**, 3280–3284 (1988).
19. E. Chin, J. E. Goodby, J. S. Patel, J. M. Gearey and T. M. Leslie, *Mol. Cryst. Liq. Cryst.*, **146**, 325–339 (1987).
20. T. Kitamura, A. Mukoh, M. Isogai, T. Inukai, K. Furukawa and K. Terashima, *Mol. Cryst. Liq. Cryst.*, **136**, 167–173 (1986).
21. Consider a one dimensional system with 3 states, g+, t, and g−. When these three states are equally populated the fraction of g states is 2/3 and the entropy is Rln3. If the energy of the t state is raised so only the g states are populated, the fraction of g states is now 1.0, but the entropy is now Rln2.
22. A. C. Griffin and J. E. Johnson, Eds., "Liquid Crystals and Ordered Fluids," **4**, pp. 1, (Plenum Press, New York, 1982).
23. T. Inukai, S. Saitoh, H. Inoue, K. Miyazawa, K. Terashima and K. Furukawa, *Mol. Cryst. Liq. Cryst.*, **141**, 251–266 (1986).
24. D. Coates, *Liq. Cryst.*, **2**, 63–71 (1987).
25. A. C. Griffin and J. E. Johnson, Eds., "Liquid Crystals and Ordered Fuids," **4**, pp. 100, (Plenum Press, New York, 1982).
26. Z. Jedlinski, J. Franek, A. Kulczycki, A. Sirigu and C. Carfagna. *Macromolecules*, **22**, 1600–1603 (1989).
27. E. Galbiati and G. Zerbi, *J. Chem. Phys.*, **84**, 3509–3518 (1986).
28. E. Fanelli, S. Melone, G. Torquati, V. G. K. M. Pisipati and N. V. S. Rao, *Mol. Cryst. Liq. Cryst.*, **146**, 235–250 (1987).
29. J. Szabon, W. Pilz and H. D. Koswig, *Crystal Res. Technol.*, **18**, 519–525 (1983).
30. P. J. Bos, A. Shetty, J. W. Doane and M. E. Neubert, *J. Chem. Phys.*, **73**, 733–743 (1980).
31. R. F. Bryan, A. J. Leadbetter, A. I. Mehta and P. A. Tucker, *Mol. Cryst. Liq. Cryst.*, **104**, 257–264 (1984).
32. J. Watanabe and R. Krigbaum, *Macromolecules*, **17**, 2288–2295 (1984).
33. QCPE 351, Quantum Chemistry Program Exchange, Indiana University, Bloomington, Indiana. The version was MNDO 2.0. Source code for input was modified to generate trial conformers from prior conformers.
34. Several dozen starting geometries were needed to produce convergence to the desired conformers. The keyword PRECISE was not used, although full geometric relaxation was permitted. Many different starting geometries led to the same final geometry. Geometries with nearly identical locations for the terminal carbon were deleted. It may be that some of the points finally selected are alternate sides of wells too shallow to force further iteration.
35. E. T. Samulsky, *J. Chem. Soc. Faraday Discuss.*, **79**, 7–20 (1985).
36. Work performed in this laboratory.
37. T. G. Adams and R. Sinta, *Mol. Cryst. Liq. Cryst.*, **177**, 145–153 (1989).
38. T. G. Adams, W. Cumming and R. Sinta, *Mol. Cryst. Liq. Cryst.*, **182B**, 257–267 (1990).
39. Y. Haramoto and H. Kamaguawa, *Chem. Letters.*, 755–758 (1987) for the compound (t)-4-[(2-methylbutyloxycarbonyl)phenyl]4-(5-undecan-1,3-dioxan-3-yl) benzoate.
40. Purchased from PCR Inc., P.O. Box 1466, Gainesville, Florida 32602.
41. Y. Hirai, T. Fujii, K. Koto, K. Suzuki, M. Yoshida, H. Yokokura, S. Hattori, A. Mukon, and M. Sato, U.S. Patent 4,564,694 (1986).